

Synthesis and characterization of a new layered lead borate

Guo-Ming Wang, Yan-Qiong Sun, Guo-Yu Yang*

State Key Laboratory of Structural Chemistry, Fujian Institute of Research on the Structure of Matter, Chinese Academy of Sciences, Fuzhou, Fujian 350002, China

Received 6 September 2005; received in revised form 18 October 2005; accepted 23 October 2005
Available online 23 November 2005

Abstract

A new lead borate, $\text{Pb}[\text{B}_8\text{O}_{11}(\text{OH})_4]$, has been hydrothermally synthesized and structurally characterized by single crystal X-ray diffraction, FTIR, powder X-ray diffraction and thermogravimetric analysis. The compound crystallizes in the monoclinic system, space group $P2_1/n$ (No. 14), $a = 7.9081(2)$ Å, $b = 14.0248(3)$ Å, $c = 9.9910(3)$ Å, $\beta = 90.327(2)$ °, $V = 1108.08(5)$ Å³, and $Z = 4$. The structure consists of layers of 9-membered borate rings enclosing Pb^{2+} cations. Adjacent borate layers are interconnected via ionic $\text{Pb}-\text{O}$ bonds and hydrogen bonding to form a 3D supramolecular network.

© 2005 Elsevier Inc. All rights reserved.

Keywords: Borates; Hydrothermal synthesis; Lead borate; Crystal structure

1. Introduction

Borate materials have attracted considerable attention in the past decades due to their rich structural chemistry and potential applications in mineralogy and industry [1–5]. From the perspective of structure, a boron atom will link with either three oxygen atoms to form a triangle (BO_3) or four oxygen atoms to form a tetrahedron (BO_4). The BO_3 and BO_4 groups are generally polymerized to form polynuclear anions, including isolated rings (or cages), infinite chains, sheets and frameworks [4,6–12]. Burns et al. [2,4] have developed a comprehensive description based on fundamental building blocks (FBBs) to have a clearer nomenclature for the borates with more complicated borate anions.

So far, many borate systems with alkali metals, alkaline earth metal, rare earth and transition metal, have been widely studied. And a number of structurally complex hydrated and anhydrous boron-containing materials have been prepared by hydrothermal syntheses and high temperature solid-state syntheses. The template synthesis of borate materials is still a particularly unexplored area, though a very few cases have been reported recently

[12–17]. The introduction of hydrothermal approach into the borate system has proved to be very effective. The aim of our work is to synthesize such materials templated by inorganic species, organic agents or transition metal complexes, and we have isolated several new compounds in this system [14–17]. As part of our continuous work, we report here a new inorganic templated borate compound, $\text{Pb}[\text{B}_8\text{O}_{11}(\text{OH})_4]$, which exhibits two-dimensional borate sheets of 9-membered boron rings.

2. Experimental section

2.1. Synthesis

The title compound was synthesized hydrothermally under autogenous pressure. Typically, a mixture of $\text{Pb}(\text{CH}_3\text{COO})_2 \cdot 3\text{H}_2\text{O}$ (0.18 g), H_3BO_3 (0.18 g), pyridine (3.26 ml) and H_2O (0.54 ml) in the molar ratio of 1:6:80:60 was stirred at room temperature. The resulting gel, with a pH of 7, was sealed in a Teflon-lined autoclave and heated at 170 °C for 6 days and then cooled to room temperature. Colorless transparent needle-like crystals were recovered by filtration, washed with distilled water, and dried in air (78% yield based on boron). The X-ray powder diffraction pattern for the bulk product is in fair agreement with the pattern based on single-crystal X-ray solution in position,

*Corresponding author. Fax: +86 591 8371 0051.

E-mail address: ygy@fjirsm.ac.cn (G.-Y. Yang).

indicating the phase purity of the as-synthesized samples of the title compound (Fig. 1). The difference in reflection intensities between the simulated and experimental patterns was due to the variation in preferred orientation of the powder sample during collection of the experimental XRD data.

2.2. Characterization

Infrared spectra were obtained from a sample powder pelletized with KBr on an ABB Bomen MB 102 series FTIR spectrophotometer over a range 400–4000 cm^{−1}. Powder X-ray diffraction (XRD) data were obtained using a Philips X'Pert-MPD diffractometer with $\text{CuK}\alpha_1$ radiation ($\lambda = 1.54056 \text{ \AA}$). The thermogravimetric analysis (TGA) was performed on a Mettler Toledo TGA/SDTA 851e analyzer in N_2 atmosphere with a heating rate of 10 °C/min.

2.3. Determination of crystal structure

A suitable single crystal of as-synthesized compound with the dimensions of $0.50 \times 0.10 \times 0.04 \text{ mm}^3$ was carefully selected under an optical microscope and glued to thin glass fiber with epoxy resin. Crystal structure determination by X-ray diffraction was performed on a Siemens SMART CCD diffractometer with graphite-monochromated $\text{MoK}\alpha$ ($\lambda = 0.71069 \text{ \AA}$) in the ω scanning mode at room temperature. An empirical absorption correction was applied using the SADABS program [18]. The structure was solved by direct methods using SHELXS-97 [19]. The lead atom was first located, and the boron and oxygen atoms were found in the successive Fourier difference maps. All the hydrogen atoms were placed geometrically. The structures were refined on F^2 by full-matrix least-

squares methods using the SHELXL-97 program package [19]. All non-hydrogen atoms were refined anisotropically. Crystallographic data and final atomic coordinates for the title compound are presented in Tables 1 and 2,

Table 1
Crystal data and structure refinement for $\text{Pb}[\text{B}_8\text{O}_{11}(\text{OH})_4]$

Empirical formula	$\text{H}_4\text{B}_8\text{O}_{15}\text{Pb}$
Formula weight	537.70
Crystal system	Monoclinic
Space group	$P2_1/n$
$a/\text{\AA}$	7.9081(2)
$b/\text{\AA}$	14.0248(3)
$c/\text{\AA}$	9.9910(3)
$\beta/^\circ$	90.327(2)
$V/\text{\AA}^3$	1108.08(5)
Z	4
$D_c/\text{g cm}^{-3}$	3.223
$\mu(\text{MoK}\alpha)/\text{mm}^{-1}$	15.321
Reflection collected	3567
Independent reflections	1910
Parameters refined	217
θ range for data collection/°	2.50–25.02
Limiting indices	$-5 \leq h \leq 9, -16 \leq k \leq 10, -11 \leq l \leq 11$
Goodness-of-fit on F^2	1.147
Final R_1 , $wR_2[I > 2\sigma(I)]$	0.0609, 0.1216
Largest diff. peak and hole (e \AA^{-3})	2.562 and -2.256

Table 2
Final atomic coordinates ($\times 10^4$) and equivalent thermal isotropic displacement U_{eq} ($\text{\AA}^2 \times 10^3$) with e.s.d.'s in parentheses of $\text{Pb}[\text{B}_8\text{O}_{11}(\text{OH})_4]$

Atoms	x	y	z	U_{eq}^{a}
Pb	1166(1)	8326(1)	8756(1)	16(1)
B(1)	2630(20)	9649(13)	3717(18)	15(4)
B(2)	1998(19)	8208(12)	5101(16)	9(3)
B(3)	2010(19)	8146(11)	2497(15)	6(3)
B(4)	-605(19)	7495(11)	6126(17)	7(3)
B(5)	99(19)	6983(11)	3849(15)	6(3)
B(6)	-560(20)	7413(11)	1472(17)	8(3)
B(7)	1870(20)	5677(12)	5018(17)	12(3)
B(8)	2080(20)	5733(15)	7522(18)	18(4)
O(1)	3053(15)	10593(8)	3755(12)	24(3)
O(2)	2331(14)	9227(8)	4917(11)	19(2)
O(3)	2514(14)	9141(8)	2566(11)	14(2)
O(4)	1210(12)	7853(7)	3790(10)	9(2)
O(5)	822(12)	8008(8)	1404(10)	12(2)
O(6)	3523(12)	7541(7)	2274(10)	9(2)
O(7)	3586(13)	7689(8)	5283(10)	14(2)
O(8)	822(12)	8080(7)	6167(10)	10(2)
O(9)	-1067(12)	7075(7)	4951(10)	10(2)
O(10)	-926(12)	6923(7)	2617(10)	9(2)
O(11)	1123(13)	6120(8)	3931(10)	14(2)
O(12)	2892(15)	4917(9)	4857(11)	27(3)
O(13)	1581(14)	6059(9)	6300(11)	21(3)
O(14)	1610(15)	6323(8)	8578(12)	23(3)
O(15)	3009(15)	4938(9)	7671(11)	26(3)

^a U_{eq} is defined as one third of the trace of the orthogonalized U_{ij} tensor.

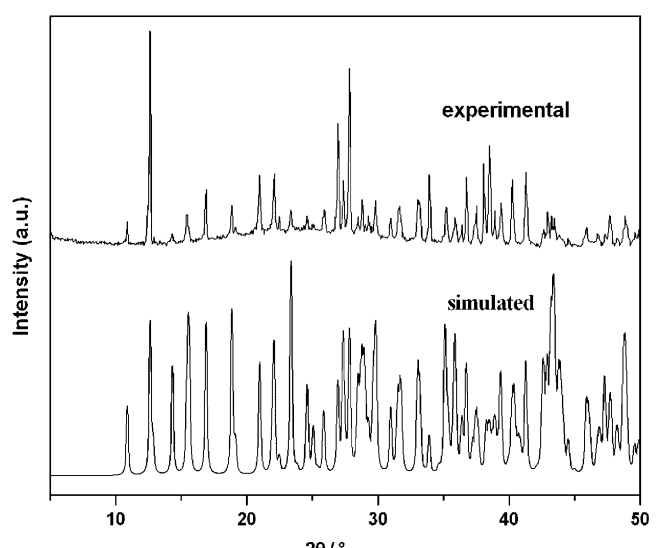
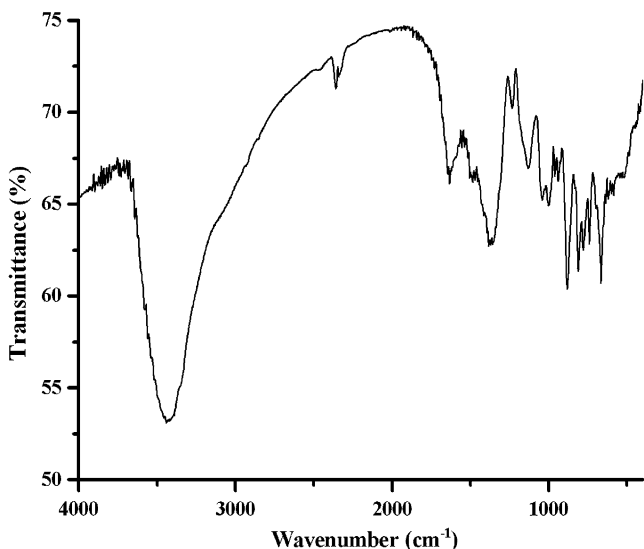
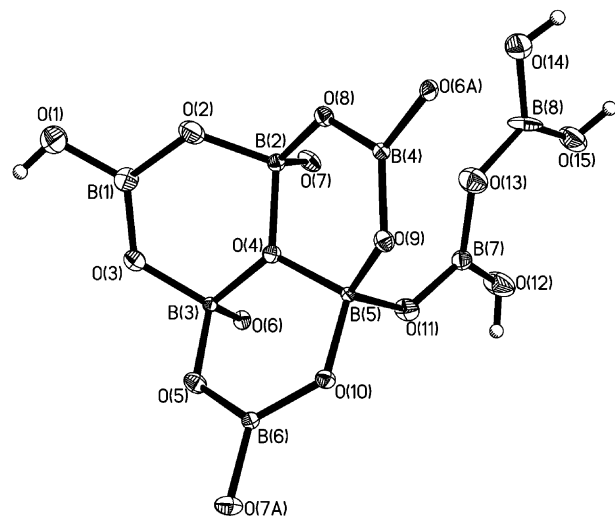


Fig. 1. Experimental and simulated X-ray powder diffraction pattern of $\text{Pb}[\text{B}_8\text{O}_{11}(\text{OH})_4]$.

Fig. 2. IR spectrum of $\text{Pb}[\text{B}_8\text{O}_{11}(\text{OH})_4]$.Fig. 3. The fundamental building block of $\text{Pb}[\text{B}_8\text{O}_{11}(\text{OH})_4]$.

respectively. CCDC 283033 or CSD 391339 contains the supplementary crystallographic data for this paper.

The highest peaks in the final difference map (2.56 eÅ^{-3}) are near the Pb atom. Relatively high residual electron densities are not unusual for Pb-containing materials as observed previously [20,22].

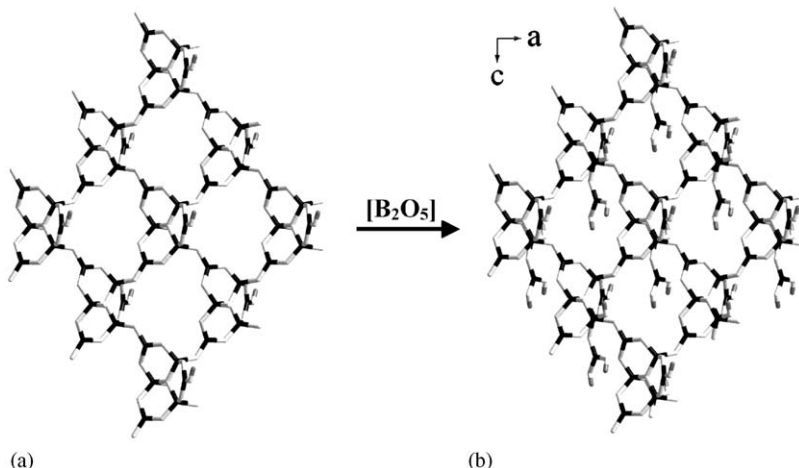
3. Results and discussion

3.1. Infrared (IR) spectrum

The FTIR spectrum of the title compound is shown in Fig. 2. The strong bands at about 1370 cm^{-1} in the spectrum are consistent with the existence of trigonally coordinated boron, while the bands at the region of 1120 – 810 cm^{-1} are characteristic of tetrahedral boron [21]. In addition, the stretching vibration of the O–H is observed at $\sim 3440 \text{ cm}^{-1}$.

3.2. Crystal structure

The asymmetric unit of the title compound contains 24 independent non-hydrogen atoms, including one lead atom, eight boron atoms and 15 oxygen atoms. The borate polyanion $[\text{B}_8\text{O}_{11}(\text{OH})_4]^{2-}$ (Fig. 3), as found only in strontioborite $\text{Sr}[\text{B}_8\text{O}_{11}(\text{OH})_4]$ [4], is the basic structural unit of the title compound. It is constituted of five BO_3 groups (triangular boron: Δ) and three BO_4 groups (tetrahedral boron: \square), which can be written as $5\Delta 3\square:[\phi]\langle\Delta 2\square\rangle|\langle\Delta 2\square\rangle|\langle\Delta 2\square\rangle|2\Delta$ with the help of the conception of FBBs after Burns et al. [2,4]. Three $\langle\Delta 2\square\rangle$ rings are linked by sharing tetrahedra. Each ring shares one tetrahedron with the adjacent two rings, generating a $[\text{B}_6\text{O}_{13}]$ unit of three triangles and three tetrahedra in which the three tetrahedra link together via an unusual O(4) atom. The remaining 2Δ units, a diborate $[\text{B}_2\text{O}_5]$ group, are attached to the above $[\text{B}_6\text{O}_{13}]$ unit

Fig. 4. (a) Layer of 9-membered boron rings constructed from $[\text{B}_6\text{O}_{13}]$ cluster. (b) View of the buckled $[\text{B}_6\text{O}_{13}]$ sheet decorated with the $[\text{B}_2\text{O}_5]$ groups along the b -axis (color scheme: B, dark gray; O, white).

by sharing a common oxygen atom. The B–O bond lengths and O–B–O bond angles are in the range of 1.343(2)–1.531(2) Å and 106.4(2)–125.7(2)°, which are in good agreement with those reported previously for other lead borate compounds [22].

The structure of the title compound can be described as borate layers, stacked one over another to form the polyborate structures. As shown in Fig. 4a, layers of 9-membered boron rings are constructed from the $[B_6O_{13}]$ groups, which are linked together through exocyclic oxygen atoms [O(6), O(7)] to neighboring units. The $[B_2O_5]$ groups, however, act as the decoration of the sheets and protrude alternately above and below the 9-membered boron rings of the borate layers (Fig. 4b). It is noteworthy that such 9-membered window systems have also been found in some lamellar or microporous germanates [23–25], which shows that 9-membered ring is a common structural geometry existing in different systems. The inorganic template Pb^{2+} cations, as shown in Fig. 5, residing at the center of the 9-membered boron rings, compensate the negative charges of the layers and they are believed to be responsible for holding the layers structures together mainly through bonding with oxygen atoms of the borate polyanions. The environment of the Pb atom consists

Table 3
Details of hydrogen bonds for $Pb[B_8O_{11}(OH)_4]^2$ ^a

D–H…A	<i>d</i> (D–H) (Å)	<i>d</i> (H…A) (Å)	<i>d</i> (D…A) (Å)	\angle (DHA) (deg)
O(1)–H(1A)…O(11) [#9]	0.82	2.04	2.86(2)	175(1)
O(12)–H(12A)…O(3) [#10]	0.82	1.85	2.67(2)	177(1)
O(14)–H(14A)…O(1) [#8]	0.82	2.06	2.87(2)	168(1)
O(15)–H(15A)…O(2) [#8]	0.82	1.80	2.62(2)	178(1)

Symmetry transformations used to generate equivalent atoms: #8 $-x+1/2, y-1/2, -z+3/2$; #9 $-x+1/2, y+1/2, -z+1/2$; #10 $-x+1/2, y-1/2, -z+1/2$.

^aD and A signify donor and acceptor oxygens, respectively.

of six oxygen atoms with the Pb–O distances in the range of 2.550(2)–2.753(2) Å, which are in accordance with those found in other lead-containing compounds [22]. In addition, there exists weak hydrogen bonding interactions between adjacent layers with O…O from 2.62(2) to 2.87(2) Å (Table 3). The connectivity of the H-bonds and Pb–O bonds gives rise to a 3D supramolecular network, as shown in Fig. 6.

3.3. Thermal property

Thermogravimetric (TG) analysis (Fig. 7), carried out in a flow of N_2 , showed that the structure of the title compound remains stable up to 400 °C. On further heating, a sharp weight loss of 7.23% occurred in the range of 400–810 °C, which was attributed to the removal of the dehydration of hydroxyls (calcd: 6.70%). The residue after the calcination for the title compound is amorphous but has not been characterized further.

4. Conclusion

In summary, the synthesis, crystal structure, and thermal properties of a new layered lead borate, $Pb[B_8O_{11}(OH)_4]^2$, has been described. The structure consists of $[B_8O_{11}(OH)_4]^{2-}$ polyanions, which are linked together to form borate layers of 9-membered boron rings. The inorganic template Pb^{2+} cations, reside at the center of the 9-membered boron rings and compensate the negative charges of the layers. Adjacent borate layers are interconnected via ionic Pb–O bonds and hydrogen bonding to form a 3D supramolecular network. To the best of our knowledge, the title compound is the first instance of artificial metal borate containing $[B_8O_{11}(OH)_4]^{2-}$ polyanion except a borate mineral of $Sr[B_8O_{11}(OH)_4]$ [4]. In addition, compared with traditionally high temperature solid-state synthesis, the hydrothermal approach has also been proved to be very effective in the construction of novel borates.

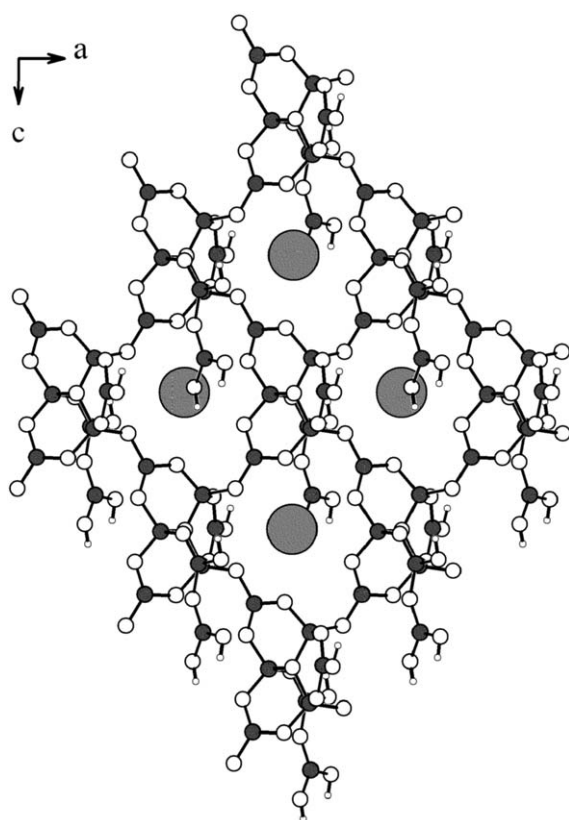


Fig. 5. View of layers of 9-membered boron rings enclosing Pb^{2+} cations. Color code: B, dark gray; O, white; Pb, light gray.

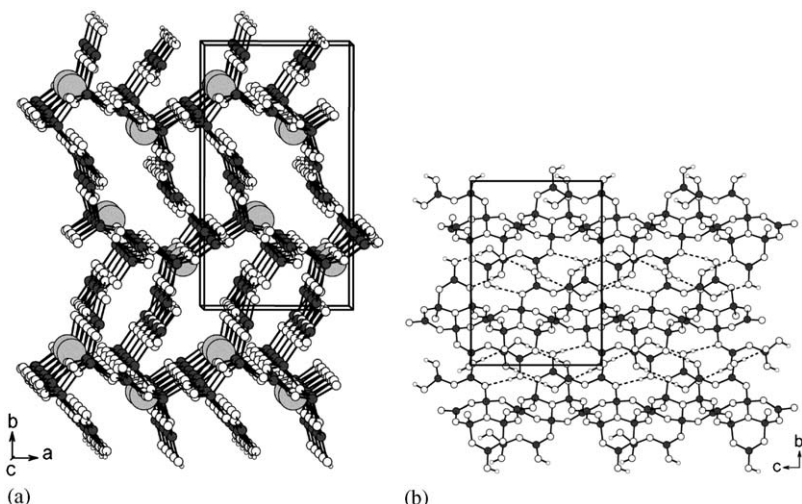


Fig. 6. (a) View of the packing structure of $\text{Pb}[\text{B}_8\text{O}_{11}(\text{OH})_4]$ along the approximate c -axis, showing the linkages of the adjacent layers through the Pb atoms. (b) View of the packing structure of $\text{Pb}[\text{B}_8\text{O}_{11}(\text{OH})_4]$ along the a -axis, showing the linkages of the H-bonds between adjacent layers. The Pb atoms are omitted for clarity. Color code: B, dark gray; O, white; Pb, light gray.

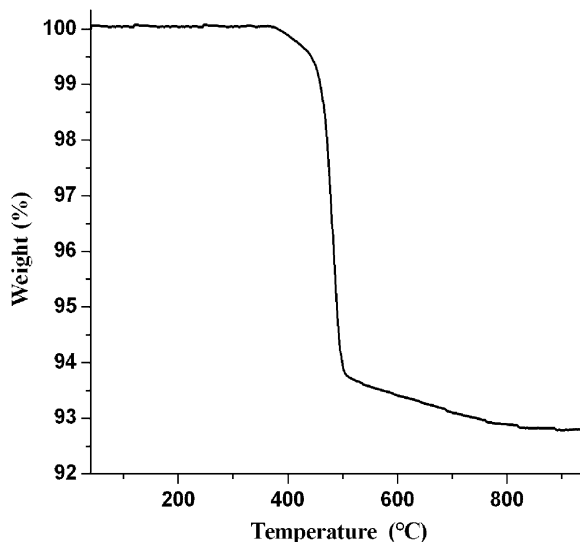


Fig. 7. TG curve of $\text{Pb}[\text{B}_8\text{O}_{11}(\text{OH})_4]$.

Acknowledgment

This work was supported by the NNSF of China (Grant Nos. 20171045, 20271050 and 20473093), the Talents Program of Chinese Academy of Sciences, and the NSF of Fujian Province (Grant No. E0510030 and E0210029).

References

- [1] C.L. Christ, J.R. Clark, *Phys. Chem. Miner.* 2 (1977) 59.
- [2] P.C. Burns, J.D. Grice, F.C. Hawthorne, *Can. Mineral.* 33 (1995) 1131.
- [3] P.C. Burns, *Can. Mineral.* 33 (1995) 1167.
- [4] J.D. Grice, P.C. Burns, F.C. Hawthorne, *Can. Mineral.* 37 (1999) 731.
- [5] C. Chen, Y. Wang, B. Wu, K. Wu, W. Zeng, L. Yu, *Nature* 373 (1995) 322.
- [6] M. Touboul, N. Penin, G. Nowogrocki, *Solid State Sci.* 5 (2003) 1327.
- [7] M. Touboul, N. Penin, G. Nowogrocki, *J. Solid State Chem.* 143 (1999) 260.
- [8] D.M. Schubert, F. Alam, M.Z. Visi, C.B. Knobler, *Chem. Mater.* 15 (2003) 866.
- [9] Z. Yu, Z. Shi, Y. Jiang, H. Yuan, J. Chen, *Chem. Mater.* 14 (2002) 1314.
- [10] N. Penin, M. Touboul, G. Nowogrocki, *J. Solid State Chem.* 168 (2002) 316.
- [11] H. Huppertz, B. von der Eltz, *J. Am. Chem. Soc.* 24 (2004) 9376.
- [12] D.M. Schubert, M.Z. Visi, C.B. Knobler, *Inorg. Chem.* 39 (2000) 2250.
- [13] H.H.Y. Sung, M.M. Wu, I.D. Williams, *Inorg. Chem. Commun.* 3 (2000) 401.
- [14] H.-X. Zhang, S.-T. Zheng, G.-Y. Yang, *Acta Crystallogr. C* 60 (2004) m241.
- [15] H.-X. Zhang, J. Zhang, S.-T. Zheng, G.-Y. Yang, *Cryst. Growth Design* 5 (2005) 157.
- [16] G.-M. Wang, Y.-Q. Sun, G.-Y. Yang, *J. Solid State Chem.* 177 (2004) 4648.
- [17] G.-M. Wang, Y.-Q. Sun, G.-Y. Yang, *J. Solid State Chem.* 178 (2005) 729.
- [18] G.M. Sheldrick, A program for the Siemens Area Detector Absorption correction, University of Gottingen, 1997.
- [19] (a) G.M. Sheldrick, *SHELXS97 Program for Solution of Crystal Structures*, University of Göttingen, Göttingen, Germany, 1997; (b) G.M. Sheldrick, *SHELXL97 Program for Solution of Crystal Structures*, University of Göttingen, Germany, 1997.
- [20] (a) S. Norberg, G. Svensson, J. Albertsson, *Acta Crystallogr. C* 55 (1999) 356; (b) J. Barbier, D. Levy, *Acta Crystallogr. C* 54 (1998) 2; (c) F. Kubel, H. Hagemann, H. Bill, *J. Solid State Chem.* 149 (2000) 56.
- [21] (a) C.E. Weir, *J. Res. Nafl. Bur. Stand. A* 70A (1966) 153; (b) C.E. Weir, R. Schroeder, *J. Res. Nafl. Bur. Stand. A* 68A (1964) 465; (c) J. Krogh-Moe, *Phys. Chem. Glasses* 6 (1965) 46.
- [22] (a) J. Krogh-Moe, P.S. Wold-Hansen, *Acta Crystallogr. B* 29 (1973) 2242; (b) H.H. Grube, *Fortschr. Mineral. Beih.* 59 (1981) 58; (c) D.L. Corker, A.M. Glazer, *Acta Crystallogr. B* 52 (1996) 260;

- (d) E.L. Belokoneva, O.V. Dimitrova, T.A. Korchemkina, S.Y. Stefanovich, *Kristallografiya* 43 (1998) 864;
- (e) R.K. Rastsvetaeva, A.V. Araksheeva, D.Y. Pushcharovsky, S.A. Vinogradova, O.V. Dimitrova, S.Y. Stefanovich, *Z. Kristallogr.* 213 (1998) 240;
- (f) Z.T. Yu, Z. Shi, Y.S. Jiang, H.M. Yuan, J.S. Chen, *Chem. Mater.* 14 (2002) 1314.
- [23] X. Bu, P. Feng, T.E. Gier, D. Zhao, G.D. Stucky, *J. Am. Chem. Soc.* 120 (1998) 13389.
- [24] P. Feng, X. Bu, G.D. Stucky, *Chem. Mater.* 11 (1999) 3025.
- [25] T. Conradsson, X. Zou, M.S. Dadachov, *Inorg. Chem.* 39 (2000) 1716.